ELSEVIER

Materials Chemistry and Physics 46 (1996) 36–42

MATERIALS CHEMISTRY AND PHYSICS

The bonding behavior of DP-Bioglass and bone tissue

Feng-Huei Lin [a], Chun-Hsu Yao [b], Chin-Wang Huang [b], Hwa-Chang Liu [c], Jui-Sheng Sun *, [c], Cheng-Yi Wang [a]

[a] *Center for Biomedical Engineering, College of Medicine, National Taiwan University, Taipei, Taiwan, ROC*
[b] *Department of Chemistry, Chung-Yuan University, Chun-Li, Taiwan, ROC*
[c] *Department of Orthopaedics, College of Medicine, National Taiwan University, Taipei, Taiwan, ROC*

Received 1 June 1995; accepted 27 November 1995

Abstract

There are many reports on the surface reactions of surface-active ceramics. A Ca–P-rich layer was found on the surface of these bioactive ceramics implanted in bone tissue, a chemical bond having been established between the mineralized matrix of the bone and the apatite layer of the bioactive ceramic. It has been reported that the direct bonding of bone to DP-Bioglass was due to the deposition and subsequent mineralization of organic bone matrix at the outer layer of the implant. Thus the strength of the bonding of DP-Bioglass with bone structure is expected to be such that it will overcome the fixing problems of joint replacement and improve the long-term performance of prostheses if the bioactive glass is coated onto alloys or stainless steel. In this study, DP-Bioglass was pressed into a steel disc, 6 mm in diameter and 5 mm thick, under a hydrostatic pressure of 270 MPa, and then sintered at 810 °C for 2 hours. The DP-Bioglass discs were implanted into the condyle area of mature male rabbits for 2, 4, 8, 16 and 32 weeks. The failure load, when an implant detached from the bone or when the bone itself broke, was measured by a push-out test. Sintered hydroxyapatite bioceramic was used in a control group and the results were compared with those using DP-Bioglass. The histological evaluation and histomorphometric investigation are described in the study to demonstrate the bonding behavior between DP-Bioglass and bone tissue.

Keywords: Bone graft; Bioceramics; Bioglass; Bonding behavior

1. Introduction

Insertion of a biomaterial in a living tissue tends to create an artificial interface between the living tissue and the biomaterial. An ideal interface between an implant and the surrounding tissue should behave in the same way as a theoretical plane present at the same place in the healthy tissue. When an implant and tissue are brought into contact, a mutual interaction may be initiated, i.e. the implant may induce changes in the biological system, which may in turn, via surface reactions, induce changes in the implant material [1,2]. At the interface, primary reactions will take place on a molecular scale, such as dissolution of ions from the material, protein adsorption and desorption, denaturing of proteins, etc. The processes may induce secondary reactions far away from the interface [3].

The clinical use of artificial implants in the field of orthopedic surgery has greatly increased in the last decade and will apparently continue to increase in the future. Total hip replacement has widely been accepted as the treatment of choice for elderly patients with advanced arthritic disorders of the hip. In active young adults, however, nearly 60% of the total hip replacements had real or potential loosening problems at the 5-year follow-up. In order to obtain satisfactory long-term results of bone or joint replacements, especially for those who are young and active, an alternative method for fixing the prosthesis without using methylmethacrylate, whose monomer has been reported to be tissue cytotoxic, should be developed [4].

DP-Bioglass has been reported to present a high mechanical strength and form a tight chemical bond with living bone tissue [5]. Light microscopy and transmission electron microscopy showed that the direct bonding of bone to DP-Bioglass was due to the deposition and subsequent mineralization of organic bone matrix — mainly composed of collagen and mucopolysaccharides — at the outer layer of the implant. It was shown that the interface between bone and the bioactive glass was mineralized by the same process observed in primary bone formation. Between the collagen fibers and the bioactive glass, there is an amorphous zone, 800–1000 Å thick, that can be mineralized and which seems to play a special role [6–8]. The reactivity of the bioactive

* Corresponding author.

PII S0254-0584(96)01749-X

glass is the result of its solubility and the leaching of ions into the surrounding intercellular matrix. The strength of the bonding between DP-Bioglass and bone structure is expected to be great enough to overcome the fixing problems of joint replacement and improve the long-term performance of prostheses if bioactive glass is coated on alloys or stainless steel.

In this project, the authors investigate the exact bonding strength between DP-Bioglass and living bony structure. Sintered hydroxyapatite bioceramic was prepared for use as a control and the results were compared with those of DP-Bioglass. The histological evaluation and histomorphometric investigation are also described in this study to demonstrate the bonding behavior between DP-Bioglass and bone tissue.

2. Materials and methods

2.1. Materials preparation

The glass used in the study was based on the DP-Bioglass of the Na_2O-CaO-SiO_2-P_2O_5 system. A batch mixture (nominal composition: Na_2O, 8.4; CaO, 40; P_2O_5, 12; SiO_2, 39.6% (wt./wt.)) was melted in a platinum crucible at 1400 °C for 1 hour. The melting glass was poured into ice water at 0 °C to quench as glass frit. The glass frit was pulverized into grains of about 5 μm using a Spex 8000 alumina ball-mill. The glass powder was pressed into a disc, 6 mm in diameter and 5 mm thick, under a hydrostatic pressure of 270 MPa. The glass powder compact was placed on a platinum sheet and heated to 810 °C at a rate of 5 °C min^{-1} in a furnace with a SiC heating element, and then allowed to cool in the furnace after 2 hours soaking time. The sintered DP-Bioglass discs were then available for rabbit femoral lateral condyle implantation [6,9].

2.2. Preparation of sintered hydroxyapatite discs

Hydroxyapatite with the atomic ratio Ca/P = 1.58–1.67 can be obtained in the form of a loose powder by precipitation from aqueous solution. A 0.3 M H_3PO_4 aqueous solution was added dropwise to a 0.5 M, 1.5 liter $Ca(OH)_2$ solution at 70–80 °C, then stirred in a 2000 ml beaker by a propeller agitator. After the pH of the mixed solution reached about 8.5–9, the solution was left standing for 20 hours while the reaction matured at room temperature without stirring. The precipitates were removed from the mother liquor by centrifugal filtration. The synthesized powder was washed with distilled water for complete removal of free residual PO_4^{-3} and Ca^{+2} ions, and then dried at 60 °C for 3 days. The reaction equation was as follows [6,10,11]:

$$10Ca(OH)_2 + 6H_3PO_4 \xrightarrow{pH \approx 8.5-9.0} Ca_{10}(PO_4)_6(OH)_2 + 18H_2O$$

The synthesized powder was pressed into a disc, 6 mm in diameter and 5 mm thick, with a hydrostatic pressure of 270 MPa. The disc powder compacts were sintered at a temperature of 1250 °C for 1.5 hours. The sintered disc powder compacts, called sintered hydroxyapatite (SHA), were used as implants in the femoral lateral condyle of experimental animals.

2.3. Experimental procedures

2.3.1. Operation

The DP-Bioglass and SHA discs were cleaned in an acetone-filled ultrasonic cleaner for about 30 minutes and sterilized conventionally with an autoclave sterilizer at 150 °C for 1 hour. The discs were then implanted into the bilateral femoral condyle of mature male New Zealand rabbits weighing 3–3.5 kg. These animals were reared and the animal experiments carried out at the Institute of Laboratory Animals, College of Medicine, National Taiwan University.

The operations were performed in a conventional theater with the animals lying supine on an operating table. They were anesthetized with a sodium pentobarbital injection in a dose of 40 mg/kg of body weight. After shaving, disinfection and sterile draping of the operation site, the femoral condyles were exposed by means of a medial longitudinal incision. Initially, a substance defect was created by a 2 mm drill and subsequently expanded with a 5 mm drill. All the drill holes were carefully rinsed with Ringer's solution and cleaned out, so that any abraded particles formed during drilling were removed. These defects were then completely filled with the corresponding implant material. The wound was sutured atraumatically in two layers with 3.0 nylon and chromic catgut brow. The operation was performed under standard aseptic conditions [9,12].

The rabbits were sacrificed at 2, 4, 8, 16, and 32 weeks after the operation. The total number of experimental rabbits executed in the study was 30. Both legs of each rabbit were used. Six rabbits and 12 legs were examined at each time period; six legs were used as the DP-Bioglass group and six as the SHA group. These two group of discs were randomly applied to 12 legs with no one rabbit receiving the same treatment to both legs.

Polymer embedding attained particular significance through the discovery of fluorescent microscopic intravital staining with tetracycline and calcein green. The 30 rabbits harvested at the above-mentioned time periods after operation were intramuscularly injected with tetracycline (30 mg/kg) 16 and 8 days before sacrifice, and calcein green (15 mg/kg) subcutaneously 12 and 4 days before sacrifice [6,12].

2.3.2. Specimen preparation and analysis

The excised bone specimens, from which any remaining soft tissue had been removed, were fixed in 40% methanol for 24 hours. For the polymer embedding to be successful, the embedding materials must be able to penetrate the bone specimen completely. This required thorough dehydration and lipid extraction of the fixed bone specimens, performed in a graded alcohol series, for 24 hours in each solution. Several cross sections at two thicknesses, 0.2 and 2 mm, were

prepared using a diamond blade saw. The surfaces to be examined using an atomic force microscope (AFM) were prepared by polishing the 2 mm thick sections with diamond paste. The interface between the implant and the bone tissue was examined under a TopoMatrix non-contact AFM [13,14].

The thin sections, 0.2 mm thick, were cut on a milling machine with a diamond disc perpendicular to the axis of the cylinder of the embedded bone specimens. The sections were ground with graded SiC paper and polished with a diamond lap disc to 30 μm for histological evaluation under optical and fluorescent microscopes.

2.3.3. Evaluation of bonding strength

The preparation of the ceramic discs of DP-Bioglass and SHA was the same as described in the previous section. A segment of the femoral condyle containing a ceramic implant was excised. The bone tissues located on the lateral sides of the ceramic implant were carefully removed with a dental burr. The segment was then dissected transversely along the central line of the femoral condyle by making parallel cuts with a disc cutter. After such sectioning, the bone segments on either side of the implant were no longer directly connected but were joined only through the intervening implant. Extreme care was taken to remove the bone completely from the sides of the ceramic and to keep the bones and samples moist throughout this testing. A segment with the ceramic implant was placed horizontally with the condyle face up. The ceramic implant was pushed out by a push-rod connected to a Bionex testing machine at a cross-head speed of 5 mm min^{-1}. The load at which an implant detached from the bone or at which the bone broke was designated as the 'failure load'. The product of the height and circumference of the disc dissected from the segment was measured as the contact area between the implant and the condyle. The failure load divided by the contact area was calculated and was considered to reflect the bonding strength between the bone and the implant. The data were assessed by a one-way analysis of the variance using a Bonferroni *t* test [15,16].

3. Results

3.1. Bonding strength

Table 1 summarizes the bonding strength of the two implants with bone. The total number of samples was six for each group and experimental period. The bonding strength shown in Table 1 is expressed as the mean value and standard deviation. These results show that the bonding strength between the DP-Bioglass and bone is lower than that of the SHA during the first 4 weeks after operation. In the second week after operation, the DP-Bioglass group's implants were detached under a very weak load. Macroscopically, the surface separated from the bone was smooth, without any tissue attached; on observation with an AFM or optical microscope, only fibrous tissue growing around the Bioglass was observed, without any bone tissue. In contrast with the DP-Bioglass group, the SHA group showed a much stronger bonding with bone tissue.

Four weeks after the operation, however, the bonding strength of the DP-Bioglass and bone had gradually increased and was higher than that of the SHA. Sixteen weeks after operation, all the samples from the DP-Bioglass group were fractured in the area of the bony structure rather than at the interface of the implant and the bone or ceramic itself. The results reflected the fact that the strength of the interface between the DP-Bioglass and bone was higher than that of the bone tissue. In the DP-Bioglass samples, the bonding strength reached a steady state after the 16th week postoperation.

Sixteen weeks after the operation, two samples were found to have fractured at the site of the bone tissue, whereas four samples had failed at the interface of the SHA and bony structure. After 32 weeks, all the samples of the SHA group had detached in the region of the bone tissue instead of at the interface.

3.2. Histological evaluation of DP-Bioglass implantation

DP-Bioglass discs were inserted as bone substitute in 30 rabbits. Fig. 1 shows the zoom image of the DP-Bioglass–bone interface examined by AFM. There is a deep gorge between the DP-Bioglass and the bony structure. The gorge was occupied by connective tissue, the early organization of which is shown in Fig. 2. The surface of the DP-Bioglass was occasionally covered with a delicate layer of cells, which had settled directly on the DP-Bioglass surface in an epithelioid manner. These cells were bulb shaped but could not be identified with certainty as osteoblasts; they may have been preosteoblasts or osteoprogenitors. Four weeks after implantation, some marginal portions of the DP-Bioglass discs were already surrounded by regenerated bone (Fig. 3).

From AFM observations (Fig. 4), the DP-Bioglass and bony tissue had been linked up by the newly generated bone,

Table 1
Bonding strength and implantation period of the DP-Bioglass and SHA discs

Ceramic	2 weeks	4 weeks	8 weeks	16 weeks	32 weeks
DPBG	1.08 + 0.026	22.91 + 15.00	62.19 + 9.92	76.33 + 17.5	78.23 + 10.98
SHA	15.83 + 9.41	32.50 + 13.67	52.33 + 13.17	65.83 + 12.8	68.57 + 8.97

DPBG = DP-Bioglass; SHA = sintered hydroxyapatite.
$p < 0.001$ implies a significant difference between the DPBG group and the SHA group.

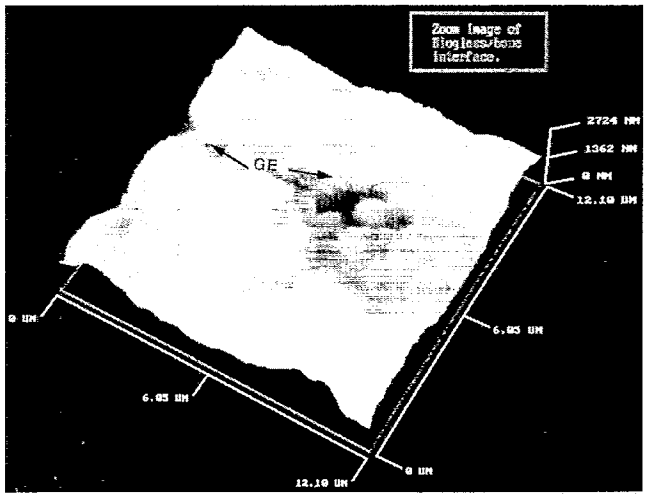

Fig. 1. Zoom image of DP-Bioglass/bone interface examined by atomic force microscope. GE, gorge.

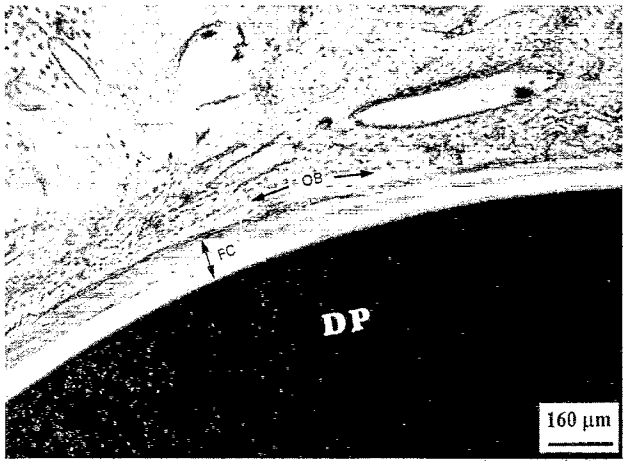

Fig. 2. Optical micrograph of DP-Bioglass disc implanted in the bone defect site 2 weeks after operation. OB, original bone; DP, DP-Bioglass; FC, connective tissue with early organization.

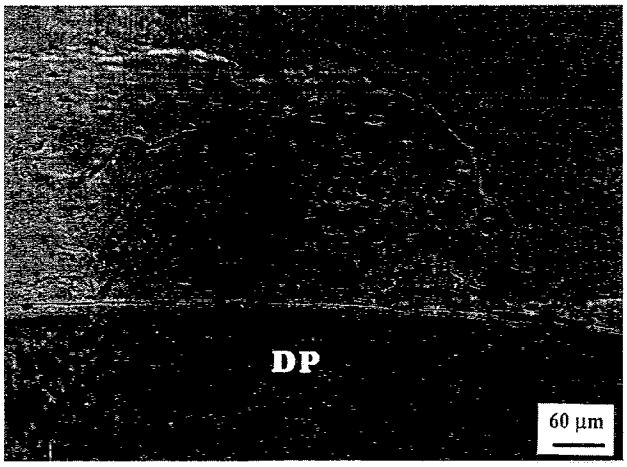

Fig. 3. After 4 weeks of implantation, some of the marginal portions of the DP-Bioglass disc already surrounded by regenerated bone. DP, DP-Bioglass; NB, newly generated bone.

with no separating fibrous tissue between them. At this stage, osteoblasts could be detected directly on the surface of the DP-Bioglass; they were embedded in the previously mineralized bony structure and would eventually develop into osteocytes.

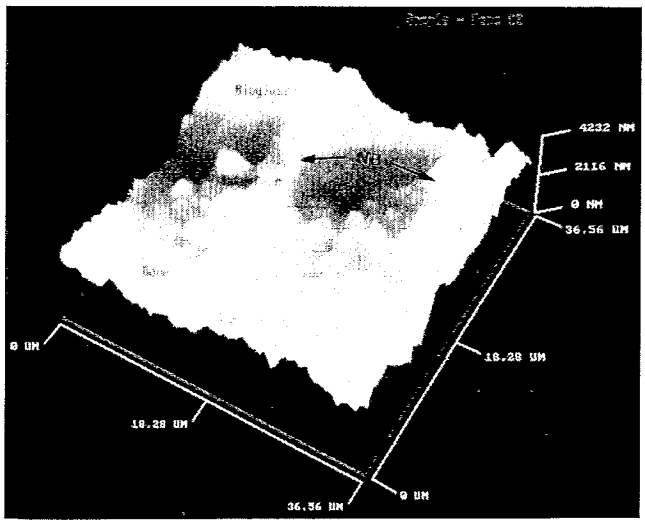

Fig. 4. DP-Bioglass and bony tissue linked up by newly generated bone with no separating fibrous tissue between them 4 weeks after operation. NB, newly generated bone.

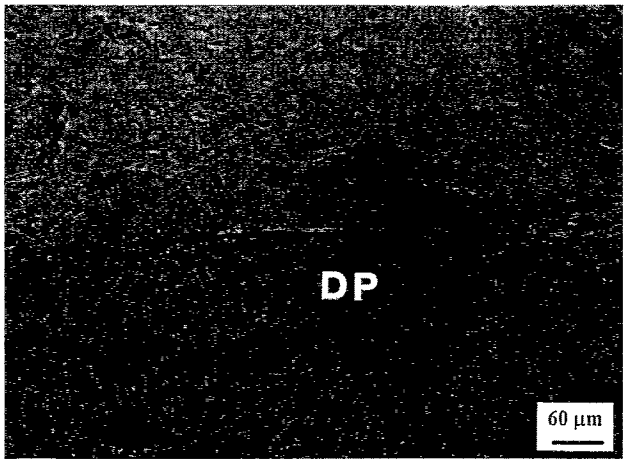

Fig. 5. Optical micrograph of DP-Bioglass disc implanted in the created defect area 8 weeks after operation. It shows not only bone regeneration directed toward the surface of the DP-Bioglass disc, but massive stimulation of osteoregeneration. DP, DP-Bioglass; NB, newly generated bone.

Eight weeks after operation, bone regeneration was almost complete. Fig. 5 shows that not only is bone regeneration directed toward the surface of the DP-Bioglass discs, but there is massive stimulation of osteoregeneration. Under a fluorescent microscope, the separate layers of regenerated bone around the DP-Bioglass were labeled with tetracycline and calcein green (Fig. 6). In this area, osteoid was present in contact with bone, and osteoblasts were seen to be arrayed in a line, indicating appositional bone formation. This process seemed to have advanced gradually from absorption of recently formed immature woven bone on the surface of the DP-Bioglass to appositional bone formation. By the 16th week, most of the area around the DP-Bioglass was covered with newly generated bone. The regenerated bone became wider and appeared more mature, but tended to decrease in quantity. The fading of the regenerated bone was in terms of biomechanical requirements and the bone remodeling proc-

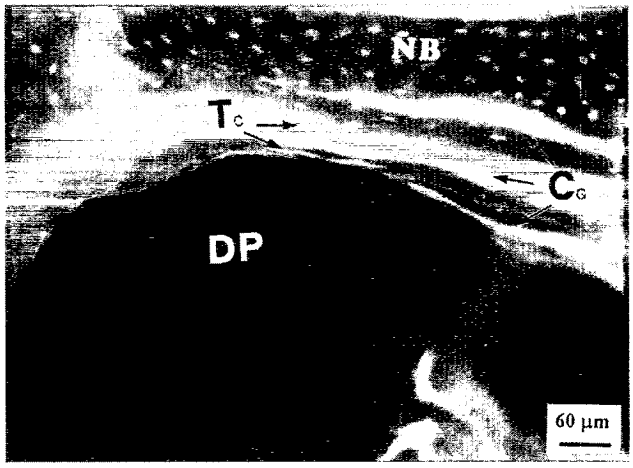

Fig. 6. Under the fluorescent microscope, laminar regeneration of bone around DP-Bioglass labelled separately in layers with tetracycline and calcein green. Tc, tetracycline; Cg, calcein green; NB, new bone; DP, DP-Bioglass.

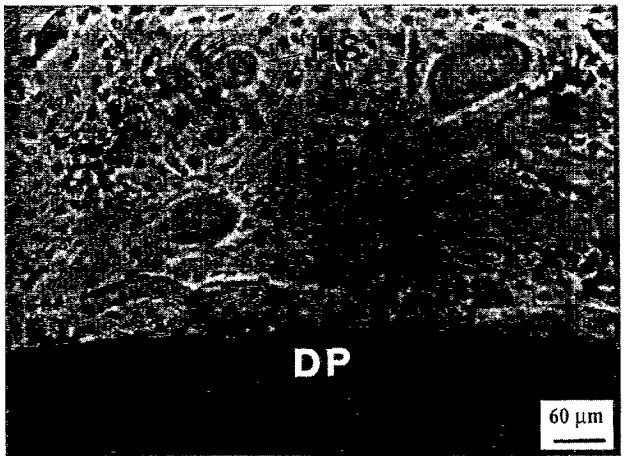

Fig. 7. The Haversian system already developed in the new bone 16 weeks after operation. HS, Haversian system; DP, DP-Bioglass.

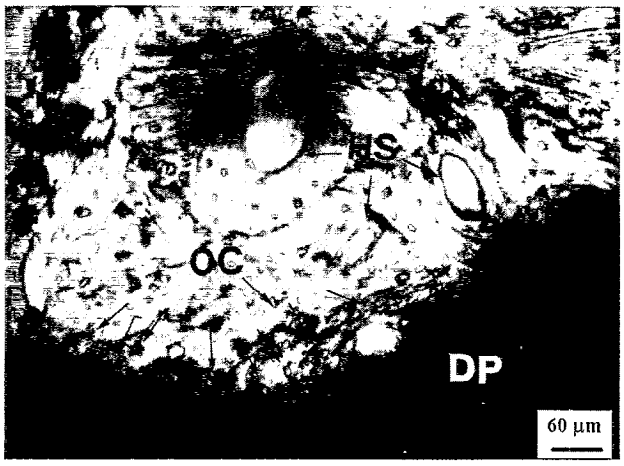

Fig. 8. Optical micrograph revealing osteocytes growing into the DP-Bioglass and penetrating into the whole material due to degradation and bioabsorption of the DP-Bioglass in the physiological environment. OC, osteocyte; DP, DP-Bioglass; HS, Haversian system.

ess. The Haversian system had already developed in the new bone area (Fig. 7).

Subsequent developments involved remodeling of the regenerated bone during the test up to 16 weeks. In this stage, the diminished area of the DP-Bioglass was attributed to its degeneration and bioabsorption in the living tissue. After 32 weeks, the bone regeneration and remodeling continued. Fig. 8 reveals that osteocytes grew into the DP-Bioglass and penetrated into the whole material due to degeneration and bioabsorption of the DP-Bioglass in the physiological environment. It was speculated that the replaced area could lead to a rough interface between the DP-Bioglass and bone tissue. Afterwards, it would result in strong bonding.

3.3. *Histological evaluation of the SHA implantation*

Fig. 9 shows the histological evaluation of the SHA discs two weeks after implantation. A large quantity of regenerated bone was already detectable on the surface of the SHA implant. Many osteoblasts were present, but there was no evidence of a defensive reaction against the implant. The existence of a stronger physiochemical bonding between the SHA surface and the regenerated bone than that of the DP-Bioglass group was suggested. Four and eight weeks after operation, a large amount of regenerated bone was seen around the SHA implant. However, osteogenesis occurred only on the superfacial portions of the SHA discs.

After 16 weeks of the test, it was observed that the size, shape, and angle of intersection of the trabeculae had been remodeled. Along the bone–implant interface, it was not uncommon to observe that the individual trabeculae had joined adjacent trabeculae to form a low-density bone contacting the implant surface, as shown in Fig. 10. Moreover, the bone density and regenerated bone area of the SHA discs were obviously much lower than those of DP-Bioglass at the same experimental period. Thirty-two weeks after operation, there was no irrefutable evidence that bone regenerated on the SHA implant had undergone biodegradation or bioabsorption; the SHA discs were still present almost in their entirety (Fig. 11), which might be the reason for the lower

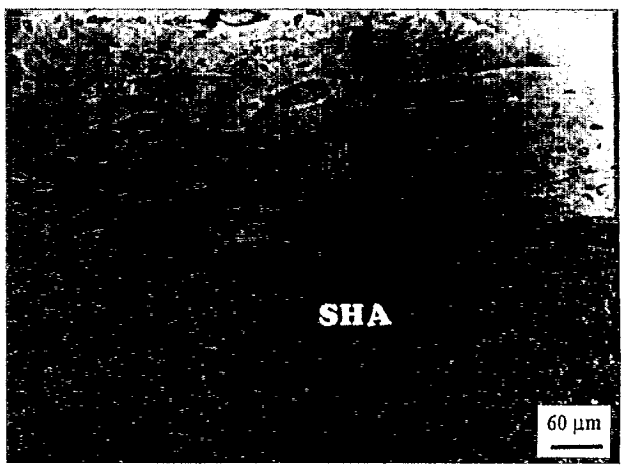

Fig. 9. Histological evaluation of the SHA disc 2 weeks after implantation. SHA, sintered hydroxyapatite; NB, newly generated bone.

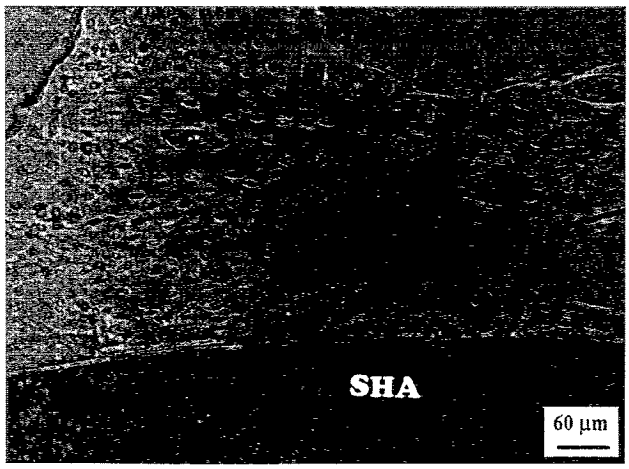

Fig. 10. Individual trabeculae joined to adjacent trabeculae to form low-density bone contacting the implant surface after the SHA disc has been implanted for 16 weeks. SHA, sintered hydroxyapatite; TB, trabeculae; NB, newly generated bone.

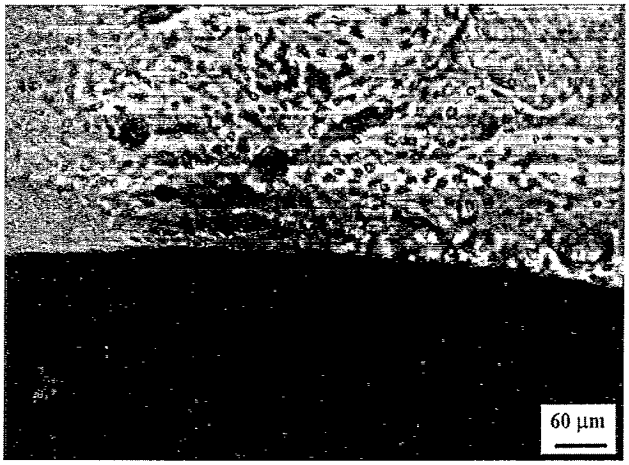

Fig. 11. SHA discs are still present almost in their entirety 32 weeks post-operation, which might be the reason for the lower bonding strength between the SHA discs and the bony structure.

bonding strength between the SHA discs and the bony structure.

4. Discussion

The bonding strength of the DP-Bioglass group was lower than that of the SHA group during the initial 4 weeks after operation, but sharply increased to a much higher bonding strength thereafter.

It is now well established that when glass with a low ratio of network former, an alkali ion content producing surface dissolution and CaO, is implanted in tissue a sequence of reactions occurs that leads to the formation of an interface capable of carrying stresses of the same order of magnitude as the ultimate strength of the tissue in which it is inserted. All the alkali ions leach out, yielding the formation of a silicon-rich layer, on top of which a Ca–P-rich layer is formed. Both diffusion from the glass as well as deposition from the extracellular fluids around the implant create this Ca–P-rich layer [15–17]. In the initial stages after the DP-Bioglass discs had been implanted, ion diffusion, Ca–P-rich layer formation and hydroxyapatite nucleation occurred on the surface, which would prolong the bonding period and weaken the bonding ability. The SHA group implants, however, have the same chemical composition as the living bone mineral so that the epitaxial process might occur directly on the surface without the nucleation process. Thus, the SHA implants bonded directly with the bone structure and demonstrated a higher bonding strength once contacted with the in vivo environment at the initial postoperative stage.

It is known that mineralization of bone involves a concentration enhancement of silicon at the mineralization front. Cell culture studies indicate that it is the combination of biologically active SiO_2 and apatite species that is responsible for inhibiting the proliferation of fibroblasts at a bioactive implant interface. Fibroblasts are put into a nonmitotic resting state when exposed to bioactive glasses. The length of mitotic arrest is a function of the surface nectin concentration of the cells and is reversible upon removal of the cells from the bioactive substrate. The mitotic arrest is preceded by substantial prolongation of the attachment and spreading time of the fibroblasts. This arresting effect is initiated immediately upon contact with the bioactive surface when the alkali exchange and SiO_2 hydrolysis and condensation reactions are dominant and precede extensive hydroxyapatite precipitation [16–19]. Consequently, biologically active silicon moieties may be the chemical source of the cellular nectin saturation effect observed on bioactive substrates [7,8,18].

The exact function of silicon in mineralization, the nature of its biological bond, and the metabolic pathway for silicon, if any, are still subject to debate. There is complete accord, however, that silicon must be present at a critical concentration if bone is to be formed. Thus, it would appear that the concurrence of SiO_2 hydrolysis and condensation with biological hydroxyapatite mineralization on bioactive glasses and glass-ceramics is in fact duplicating the natural repair or growth of bone [17]. There is no silicon contained in the SHA implant [9,16,17], consequently, an incubation period of the SHA implant is necessary to accumulate a critical silicon concentration and deposit biological hydroxyapatite on the front. During this period, biological silicon could accumulate at the surface of the SHA implant, which would delay the deposition process of biological hydroxyapatite on the surface of the implant. Such a conclusion is consistent with the transmission electron microscope studies of C. dePuyter [8,20].

If the arguments of the previous two paragraphs are correct, the bioactivity of the SHA implant should be higher than that of the DP-Bioglass during the initial four weeks after the operation; thereafter, the bioactivity of the DP-Bioglass might be higher than that of the SHA. The bioactivity is the characteristic of an implant material that allows it to form a bond with living tissues. Materials forming a nonadherent layer of fibrous tissue at the implant interface are not considered to be bioactive. The percentage of interfacial bone tissue

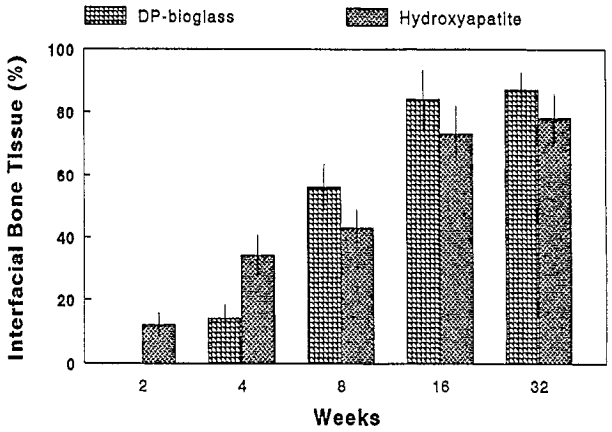

Fig. 12. Time dependence of interfacial bone tissue production for DP-Bioglass and sintered hydroxyapatite disc implants.

at the implant may reflect the material's bioactivity. The results of histological evaluation in terms of the above-defined bioactivity of the two materials are shown in Fig. 12. This figure shows the time dependence of interfacial bone tissue production for the DP-Bioglass and SHA implants. The bioactivity of the DP-Bioglass group was much lower than that of the SHA group during the initial 4 weeks after the operation; however, it increased sharply to exhibit a higher bioactivity than that of the SHA group thereafter. This is in agreement with the results of the bonding strength and in accordance with the above discussion. Moreover, the rough interface between the DP-Bioglass and the bone structure also contributed to these results.

5. Conclusions

The bonding strength of the DP-Bioglass group was lower than that of the SHA group during the initial 4 weeks posto-peration, but sharply increased and was higher than that of the SHA group thereafter. The results were in agreement with the bioactivity of the DP-Bioglass and SHA implants at different implantation periods. The bonding strength of the two implants is assumed to be related to the epitaxial growth process and biological silicon accumulation.

Acknowledgements

The authors express their gratitude to the National Science Council, Republic of China, which supported the project financially through grant No. NSC82-0402-B002-530-M09.

References

[1] T. Kitsugi, T. Yamamuro, T. Nakamura, S. Kotani, T. Kokubo and H. Takeuchi, Four calcium phosphate ceramics as bone substitutes for non-weight-bearing, *Biomaterials, 14* (3) (1993) 216–224.

[2] C.A. van Blitterswijk, J.J. Grote, W. Kuypers, C.J.G. Blok-van Hoek and W.T. Daems, Bioreactions at the tissue/hydroxyapatite interface, *Biomaterials, 6* (1985) 243–251.

[3] M. Jarcho, J.F. Kay, K.I. Gumaer, R.H. Doremus and H.P. Drobeck, Tissue, cellular and subcellular events at a bone-ceramic hydroxyapatite, *J. Bioeng., 1* (1977) 79–92.

[4] A.M. Sadegh, G.M. Luo and S.C. Cowin, Bone ingrowth: an application of the boundary element method to bone remodeling at the implant interface, *J. Biomech., 26* (2) (1993) 167–182.

[5] F.H. Lin and M.H. Hon, A study on Bioglass ceramics in the Na_2O-CaO-SiO_2-P_2O_5 system, *J. Mater. Sci., 23* (1988) 4295–4299.

[6] F.H. Lin, C.C. Lin, H.C. Liu, Y.Y. Huang, C.Y. Wang and C.M. Lu, Sintered porous DP-bioactive glass and hydroxyapatite as bone substitute, *Biomater., 15* (13) (1994) 1087–1098.

[7] L.L. Hench, R.J. Splinter, W.C. Allen and T.J. Greenlee, Bonding mechanisms at the interface of ceramic prosthetic materials, *J. Biomed. Mater. Res.*, 2 (1971) 117–141.

[8] L.L. Hench and E.C. Ethridge, *Biomaterials: An Interfacial Approach*, Biophysics and Bioengineering Ser. Vol. 4, Academic Press, New York, 1982, pp. 62–68, 126–148.

[9] F.H. Lin, Y.Y. Huang, M.H. Hon and S.C. Wu, Fabrication and biocompatibility of a porous Bioglass ceramic in a Na_2O-CaO-SiO_2-P_2O_5 system, *J. Biomed. Eng., 13* (1991) 328–334.

[10] M. Kohri, K. Miki, D.E. Waite, H. Nakajima and T. Okabe, In vitro stability of biphasic calcium phosphate ceramics, *Biomaterials, 14* (4) (1993) 299–304.

[11] M. Jarcho, Calcium phosphate ceramics as hard tissue prosthetics, *Clin. Orthop. Relat. Res., 157* (1981) 259–278.

[12] H. Westen, K.F. Muck and L. Post, Enzyme histochemistry on bone marrow sections after embedding in methacrylate at low temperature, *Histochemistry, 70* (1981) 95–98.

[13] P.E. West, Advances in scanning probe microscope applications: image resolution — effect of probe geometry, *Topometrix Tech. Note No. 91-501*, Los Angeles, March 1991.

[14] J.D. Baldeschwieler, J.M. Gill and P.E. West, The scanning probe microscope: a powerful tool for visualizing the micro world, *Am. Lab.*, (Feb.) (1991) 23–29.

[15] T. Nakamura, T. Yamamuro and S. Higashi, A new glass-ceramic for bone replacement: evaluation of its bonding to bone tissue, *J. Biomed. Mater. Res., 19* (1985) 685–698.

[16] M. Neo, S. Kotani, Y. Fujita, T. Nakamura and T. Yamamura, Differences in ceramic–bone interface between surface-active ceramics and resorbable ceramics: a study by scanning and transmission electron microscopy, *J. Biomed. Mater. Res., 26* (1992) 255–267.

[17] L.L. Hench and H.A. Paschall, Histochemical responses at a biomaterials interface, *J. Biomed. Mater. Res., 5* (1974) 49–64.

[18] C.P.A.T. Klein, K. de Groot, A.A. Driessen and H.B.M. van der Lubbe, A comparative study of different beta-whitlockite ceramics in rabbit cortical bone with regard to their biodegradation behavior, *Biomaterials, 7* (1986) 144–146.

[19] G. Daculisa, R.Z. Legeros, M. Heughebaert and I. Barbieux, Formation of carbonate-apatite crystals after implantation of calcium phosphate ceramics, *Calcif. Tissue Int., 46* (1990) 20–17.

[20] C. dePuyter, K. de Groot, P.A.E. Sillevis Smith, in J.J.C. Lee, T. Alberktsson and P.I. Branemark (eds.), *Clinical Applications of Biomaterials*, Wiley, New York, 1982, p. 237.